Electrochemical Behaviour of Titanium Based Biomaterials in Artificial Saliva

KAMEL EARAR[1], CAMELIA ANA GRIGORE[1]*, CRISTIAN BUDACU[2], LUCIA CARMEN TRINCA[3], DANIEL MARECI[4], CERASELA DORINA SINCAR[1]

[1] Dunarea de Jos University of Galati, Faculty of Medicine and Farmacy, 35 Al. I. Cuza Str., 800010, Galati, Romania

[2] Grigore T. Popa University of Medicine and Pharmacy, 16 Universitatii, Str., 700115, Iasi, Romania

[3] Ion Ionescu de la Brad University of Agricultural Sciences and Veterinary Medicine, Exact Sciences Department, 3 Mihail Sadoveanu Alley, 700490, Iasi, Romania

[4] Gheorghe Asachi Technical University of Iasi, Faculty of Chemical Engineering and Environmental Protection, 73 D. Mangeron Blvd., 700050, Iasi, Romania

In the last decade, new titanium alloys such as Ti6Al7Nb and Ti6Al7NbN have been developed in different areas of dentistry. It is known that mechanical/electrochemical interactions accelerate corrosion in implant alloys, and these interactions can be reduced by improving the modular component machining tolerances or by improving the corrosion resistance. The aim of this study was to compare the Ti6Al7Nb and Ti6Al7NbN alloys corrosion resistance in AFNOR artificial saliva. Due to the nitrogen diffusion, the Ti6Al7NbN alloy presents more pronounced grain structure than Ti6Al7Nb. In the electrochemical estimations the polarisation data were converted into instantaneous corrosion rate values (j_{corr}). The obtained passivation properties were comparable for both alloys. The EIS spectra were best fitted using an equivalent circuit (EC) which was consistent with the model of a two-layer structure for the passive film. The electrochemical and corrosion behaviour of Ti6Al7NbN increased the occurrence of the implant alloy's electrochemical degradation.

Keywords: titanium based alloys, nitrogen, artificial saliva corrosion behaviour, EIS, SEM

The corrosion process is one of the essential phenomenons that determine the biocompatibility of implant alloys. However mechanical and electrochemical interfaces interactions is an issue of continued concern in hip arthroplasty.

Commercial pure titanium and titanium alloys are used on a large scale as implant alloys due to their advantages as compared with other similar materials: chemical inertia, low specific gravity, adequate mechanical properties, toxicity absence and good biocompatibility. Corrosion resistance is determined by the formation of an adherent titanium oxide layer of reduced thickness, on titanium or titanium alloys surface. This film contains as a major compound TiO_2 with anionic gaps, which confer the *n* semiconductor character [5]. This film functions as a barrier versus the metal tendency to interact with the corrosion medium. The film formation may be enhanced by the alloying with transitional metals having d unsaturated orbitals when solid solutions with Cu, Mo, W, Nb or inter-metallic compounds with Pt, Ni are formed. The increase of the oxide film thickness conducts to the formation of a crystalline layer and of another porous layer. The last layer contains hydrated oxides with 30% water content. Corrosion of metal implants is critical because it can adversely affect biocompatibility and mechanical integrity. The biomaterial used as implant must not cause any biological reaction in the body and must be stable and retain its functional properties. Corrosion and surface film dissolution are processes responsible for introducing additional ions in the body. The material-tissue interactions [1] are influenced by the surface characteristics of titanium implants (i.e., chemistry, and morphology/texture). Thus, an important aspect of any surface modification treatment is to maintain/assure properties similar with those of titanium, when it comes of electrochemically behaviour. Any how, surface treatments that determine the depth increasing have a higher probability of wear resistance [2]. Accordingly, nitrogen diffusion hardening treatments should improve the alloy resistance to mechanical and electrochemical damage in hip prostheses.

The standard Ti6Al4V alloy was one of the first titanium biomaterial introduced in implantable components and devices (particularly for orthopaedic and osteosynthesis applications). Although this alloy is still widely used in medicine, some concern has been recently expressed over its use, since it appears that small amounts of vanadium, released in the human body, may induce possible cytotoxic effect. Thus, toxicity concerns of the alloying elements (like V from conventional Ti6Al4V alloy) determined the development of new titanium alloys with non-toxic (Nb, Zr, Ta, and Mo) elements [3-7]. Thus, the Ti6Al7Nb alloy (now commercially available, ASTM F 1295) appeared as a better alternative to Ti_6Al_4V alloy [8].

The electrochemical techniques used in the corrosion studies have their own specific advantages for addressing effectively to certain aspects of the electrochemical performance of implant materials [6].

The objective of the present research was to determine the effect of nitrogen diffusion on the corrosion behaviour of the Ti6Al7Nb alloy. Samples were examined by using the electrochemical impedance spectroscopy (EIS), and linear potentiodynamic polarization (LPP) corrosion behaviour of both titanium alloys in AFNOR artificial saliva.

Experimental part

Titanium alloys were purchased as cast presenting a rod like shape. The titanium based materials used were: Ti6Al7Nb, and $Ti_6Al_{6Z}NbN$. The Ti_6Al_7Nb alloy was diffusion-hardened (Ti_6Al_7NbN) in a nitrogen atmosphere for 8 h at 570°C and quenched at room temperature.

The microhardness was measured on an electronic AFFRI Micro HardnessTester, using a force of 200 g for 15 s.

* email: cameliaanagrigore@yahoo.com

As corrosion medium was used a solution of the aerated artificial saliva (Carter-Brugirard AFNOR/NF (French Association of Normalization). Saliva composition was: NaCl – 0.7 g/L, KCl – 1.2 g/L, $Na_2HPO_4H_2O$ – 0.26 g/L, $NaHCO_3$ – 1.5 g/L, KSCN – 0.33 g/L, carbamide – 1.35 g/L [19], and the *p*H = 8 ± 0.2.

Electrochemical measurements were carried out at room temperature immersion in AFNOR/NF artificial saliva in order that the passive film may be formed as a result of electrochemical reactions with the artificial saliva.

The titanium samples processed in cylindrical shape were mounted in a tetrafluoroethylene support, presenting a one-dimensional circular area which was exposed to corrosion and subsequent measurements.

Before experimental testing, the samples were mechanically polished with SiC abrasive paper up to a granulation number of 4000, than polished using 1 mm alumina suspension and cleaned in ethyl alcohol.

The electrochemical techniques used for the corrosion behaviour study were the potential measurements, polarization curves and electrochemical impedance spectroscopy (EIS).

The measurement was managed by a PARSTAT 4000 potentiostat controlled by a personal computer with dedicate software (Power Corr, Princeton Applied Research, Princeton, NJ, USA). A saturated calomel electrode (SCE) was used as reference and platinum as auxiliary electrode. All potential values given in this article are referred to SCE.

Electrochemical impedance spectroscopy (EIS) measurements were carried out in an open circuit potential (E_{OC}) in aerated solutions. A frequencies range from 10^{-2} to 10^5 Hz was used. The amplitude of AC potential was 10 mV with single shine wave measurements.

Linear potentiodynamic polarization was conducted at a small scan rate of the potential electrode (dE/dt = 0.5 mV/s). The corrosion current density (j_{corr}) was calculated as the slope of the potential vs. zero current potential, ZCP (in the range from –100 to +100 mV vs ZCP). As, the corrosion current densities are characterizing the metal corrosion behaviour they may evaluate how effectively a passive film protects a metal from corrosion.

The surface morphology of both titanium based alloys after linear potedynamic polarization testing was observed by scanning electron microscopy (SEM). SEM observations were made using a Quanta 200 (FEI, Hillsboro, OR, USA) operated at an accelerating voltage of 30 kV.

Results and discussions

The microhardness tests were conducted on the same flat surfaces (fig. 1).

Vickers microhardness measurements results sustained that the samples alloys formed different surface layers

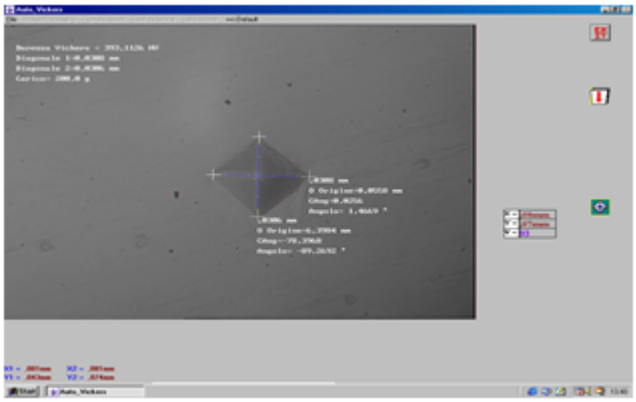

Fig.1. Representative microhardness marks on Ti6Al7NbN alloy

Table 1

AVERAGE VALUES OF VICKERS MICROHARDNESS AND DEPTHS CORRESPONDING TO THE APPLIED LOAD

Alloy	Ti6Al7Nb	Ti6Al7NbN
Load (200 grams)	265	393
Depth (μm)	5.33	4.38

(table 1). The measured average values of microhardness allowed the calculation of the depth (in mm), according to ASTM/ISO Standard Tests [12-17] by applying the formula:

$$h = \sqrt{\frac{1.854 \cdot F}{49 \cdot HV}} \qquad (1)$$

were h is the depth (thickness of the oxide layer) as a function of the applied load (Kg) and the value of the Vickers hardness (HV) obtained.

The depths corresponding values are presented in the table 1.

Electrochemical results

The corrosion resistance can be estimate by impedance method, also, known as Electrochemical Impedance Spectroscopy (EIS), a powerful tool able to perform electrochemical and corrosion investigation. EIS is capable to access phenomena whose relaxation times vary over orders of magnitudes and permits single averaging within a single experiment for obtaining high precision levels.

Figure 2-3 shows the spectra of titanium based materials immersed for different times in AFNOR artificial saliva. The Nyquist diagrams for Ti6Al7NbN alloy immersed in AFNOR artificial saliva are composed of pseudo-capacitive loops. In the case of Ti6Al7Nb alloy, the increased impedance induced a greater capacitive character.

The Bode plots exhibit a two-step aspect, indicating the presence of an oxide with two layers, i.e. a porous outer layer and a compact inner layer [18]. For Ti_6Al_7Nb alloy the

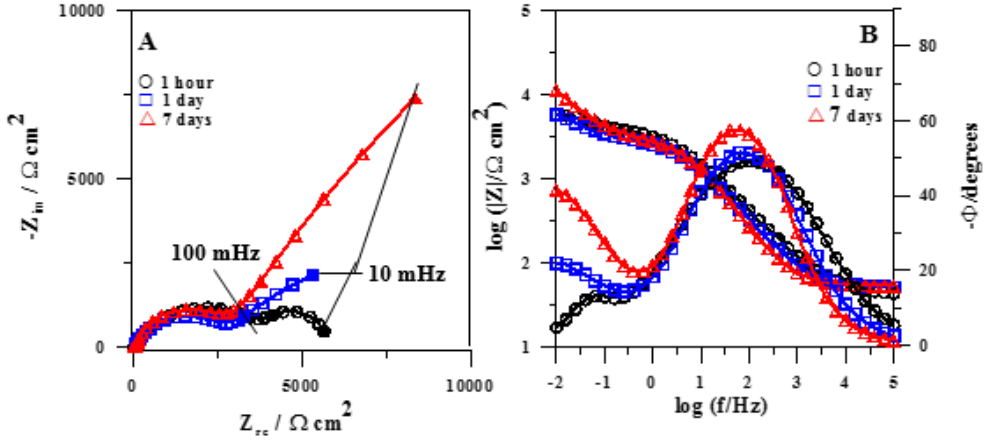

Fig. 3. Nyquist (A) and Bode (B) diagrams for Ti6Al7Nb alloy after 7 days in AFNOR artificial saliva at 37°C, measured at ZCP.

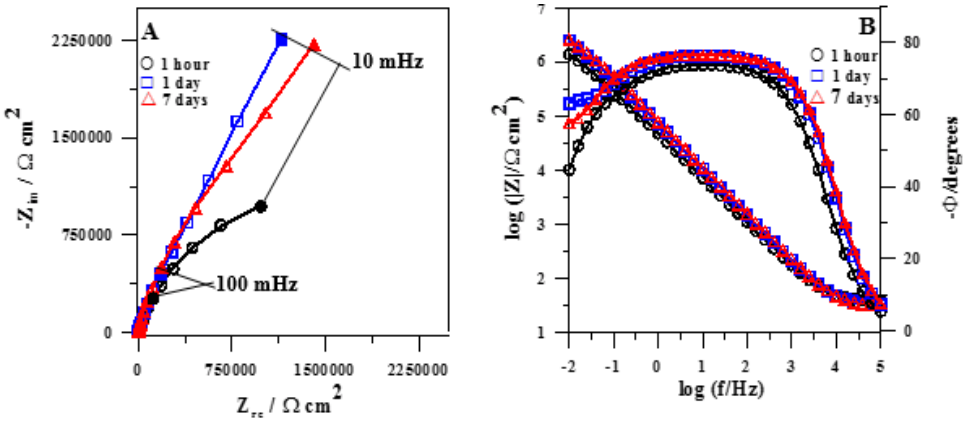

Fig. 2. Nyquist (A) and Bode (B) diagrams for Ti6Al7NbN alloy after 7 days in AFNOR artificial saliva at 37°C, measured at ZCP.

phase angle at almost -90° is characteristic for the compact oxide capacitance while in the case of Ti6Al7NbN the angle was decreased being closed to -60°, probably due to the greater thickness of the porous layer. The resulted spectra was interpreted in terms of an *equivalent circuit* (EC) with the circuit elements representing electrochemical properties of the alloy and its oxide film.

The quality of fitting to the equivalent circuit was judged firstly by the chi-square value and secondly by the error distribution vs. frequency, by comparing experimental with simulated data. The EIS experimental data were fitted and analyzed in terms of equivalent circuits (EC) using a non-linear least squares fit method (ZSimpWin 2.00 software) to obtain the relevant impedance parameters. Very good correlation was obtained between EIS data using the proposed equivalent circuit and the experimental impedance spectra, as it's evidenced by the solid lines corresponding to the fitted spectra passing through the measured data (discrete points) in figure 4.

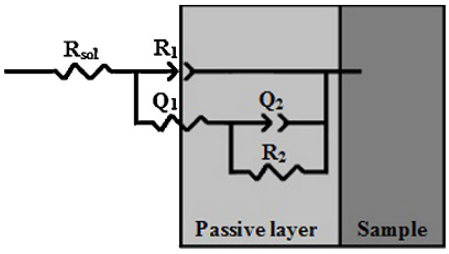

Fig. 4. Equivalent circuit (EC) used in the generation of simulated data

These equivalent circuits with two time constants are required in the case of thicker and aged oxide layers, as they would develop a duplex structure with a porous outer layer [10, 18-19].

Instead of pure capacitors, constant phase elements (CPE) were introduced in the fitting procedure to obtain good agreement between the simulated and experimental data.

The impedance of CPE is defined as:

$$Z_{CPE} = \frac{1}{Q(j\omega)^n} \quad (2)$$

where Q is the combination of properties related to both the surfaces and electroactive species independent of frequency; n is related to a slope of the lgZ vs lgf Bode–plots; ù is the angular frequency and j is imaginary number (j_2=-1). Q is an adjustable parameter used in the fitting routine: when the value of n is equal to 1, the CPE acts as a pure capacitor [19-26].

The components of the EC are: R_{sol} – ohmic resistance of the electrolyte, R_1 – resistance of the outer porous layer, R_2 – resistance of the compact inner layer, Q_1 – constant phase element of the outer porous layer, Q_2 – constant phase element of the compact inner layer.

In table 2 are presented the main parameters of the proposed equivalent circuit.

Similar value of R_{sol} for AFNOR artificial saliva (equal to 59 ± 4Ω cm^2) was observed for both titanium based alloys.

Polarization resistance (R_p) is represented by the sum of the resistance of the porous oxide layer and the compact oxide layer (R_1 + R_2) [27].

From the fitted values of table 2, some differences between the characteristics of the oxide films in both solutions are observed. In fact, the R_p values determined for Ti6Al7NbN alloy were smaller than for the Ti6Al7Nb alloy, probably because the inner film for Ti6Al7NbN alloy was less protective in the tested environment. The opposite trend was shown by the impedance parameter related to the constant phase elements Q_2, which can be related to the thickness of the inner layer. The value of the fit exponent *n* corresponds to the extent of dispersion and is attributed to surface inhomogeneity. For Ti_6Al_7Nb alloy, the values of the exponent n_2 being approximately 0.9, then can be said that Q_2 behave similarly to a pure capacitor. However, the values of the n_1 exponent were lower than those of n_2, maybe due to higher defectiveness, heterogeneity and roughness of the outer layer [28]. The Q_1 and Q_2 result values were different for either Ti_6Al_7NbN or Ti6Al7Nb alloy, fact sustaining that the porous layer formed on Ti_6Al_7NbN doesn't consist of same oxides as the compact layer.

The linear potiodynamic polarization curves are presented in figure 5. These curves were registered after 7 days of immersion of titanium alloys samples in AFNOR artificial saliva.

The Tafel slopes and the polarization resistance were evaluated from the linear polarisation curves obtained in neighbourhood of the zero current potential (ZCP), on the

Table 2
THE MAIN PARAMETERS OF THE EQUIVALENT CIRCUIT

Alloy Samples	Immersion time	R_1 (Ω cm^2)	n_1	Q_1 (S s^n cm^{-2})	R_2 (Ω cm^2)	n_2	Q_2 (S s^n cm^{-2})
Ti6Al7NbN	1hour	1.2 10^5	0.76	5.1 10^{-4}	5.9 10^5	0.79	4.7 10^{-4}
	1 day	1.4 10^5	0.76	5.0 10^{-4}	6.1 10^6	0.79	4.6 10^{-4}
	7 days	1.5 10^5	0.77	4.9 10^{-4}	6.3 10^6	0.80	4.4 10^{-4}
Ti6Al7Nb	1 hour	1.2 10^4	0.79	9.8 10^{-5}	1.2 10^6	0.85	1.3 10^{-6}
	1 day	1.4 10^4	0.79	9.8 10^{-5}	1.9 10^6	0.85	1.1 10^{-6}
	7days	1.8 10^4	0.81	9.8 10^{-5}	2.3 10^6	0.86	9.7 10^{-6}

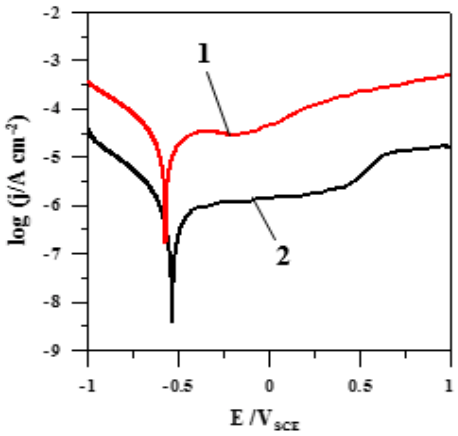

Fig. 5. Linear potentiodynamic polarization curves for the (1): Ti6Al7NbN, and (2): Ti6Al7Nb alloys after 7 days immersion in AFNOR artificial saliva solution at 37 °C. Scanning rate: 0.5 mV s^{-1}.

Table 3

CORROSION PARAMETERS (AND STANDARD DEVIATION VALUES) DETERMINED FROM THE POTENTIODYNAMIC POLARIZATION CURVES MEASURED FOR Ti6Al7Nb and Ti6Al7NbN IN AFNOR ARTIFICIAL SALIVA

Alloys	ZCP (mV_{SCE})	β_a (mV/dec)	β_c (mV/dec)	j_{corr} ($\mu A/cm^2$)
Ti6Al7Nb	-531 (14)	196 (6)	144 (6)	0.4 (0.04)
Ti6Al7NbN	-564 (11)	154 (9)	115 (9)	7.4 (0. 07)

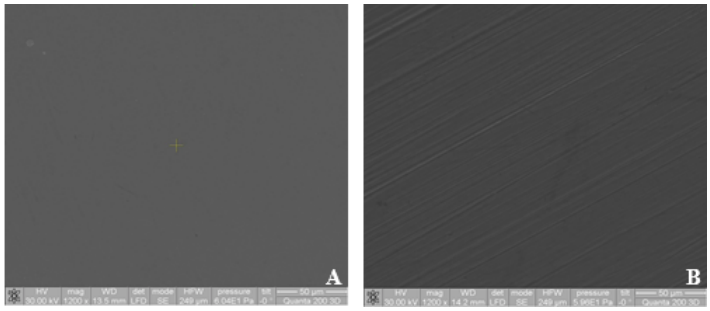

Fig. 6. SEM micrographs of: (A) Ti6Al7Nb, and Ti6Al7NbN alloy samples retrieved from AFNOR artificial saliva for 7 days after recording the potentiodynamic polarization tests at $+1V_{SCE}$

basis of the Evans diagram. These values and the instantaneous current density of the corrosion process are listed in table 3 (column 5).

The β_c values suggest that the hydrogen evolution reaction is dependent of the composition of titanium alloys. The rate of the hydrogen evolution reaction is different and descreases from Ti_6Al_7Nb to Ti_6Al_7NbN alloys. The high value of β_a in comparison with the values of β_c for both alloys indicates an anodic control in the corrosion process (table 2). The control implies the existance of a passive layer on the material surface.

The nature of the anodic linear potentiodinamic polarization curves indicates that both the samples have a similar behaviour at immersion in the AFNOR artificial saliva, but the Ti_6Al_7Nb alloy presented lower anodic current densities as compared with Ti_6Al_7NbN alloy. Also, the corrosion current densities (j_{corr}) of Ti6Al7Nb alloy were smaller than those of Ti_6Al_7NbN alloy. For both materials, the ZCP values up to 500 mV_{SCE} showed a passive behaviour.

However, TiN surface exhibit a higher degree of lubricity and a lowered coefficient of friction [29], fact reducing the probability of surface damages for Ti_6Al_7NbN, in the process of assembly in the hip prosthesis.

Figure 6 shows typical SEM images of resulting surface oxide films after polarization at $+1.0\ V_{SCE}$ in AFNOR artificial saliva for Ti_6Al_7Nb, and Ti_6Al_7NbN alloys. Neither pits nor cracks may be observed on the surface of both alloys.

Conclusions

The Vickers microhardnes values of Ti6Al7NbN alloy sample was 1.5 greater than non-nitride Ti6Al7Nb alloy. The electrochemical and corrosion behaviour of Ti6Al7NbN, and Ti6Al7Nb alloys was investigated in AFNOR artificial saliva. Density corrosion currents of both titanium based alloys showed low values. Passive behaviour was observed for either Ti_6Al_7Nb, or Ti_6Al_7NbN immersed in AFNOR artificial saliva at 37°C. The EIS spectra were best fitted using an equivalent circuit (EC) which was consistent with the model of a two-layer structure for the passive film. The results evidenced the formation of a compact oxide layer on the titanium based samples that was responsible for the corrosion protection of both titanium based alloys immersed in AFNOR artificial saliva. However, the electrochemical and corrosion behaviour of Ti6Al7NbN alloy affected the diffusion of nitrogen in Ti_6Al_7Nb alloy.

References

1. KELLER, J.C., STANFORD, C.M., WIGHTMAN, J.P., DRAUGAN, R.A., ZAHARIAS, R., J. Biomed Mat. Res. **28**, 1994, p. 939
2. SHETTY, R.H., Mechanical and corrosion properties of nitrogen diffusion hardened Ti6Al4V alloy. Editors: S.A BBROWN, I.E. LEMONS, Medical applications of titanium and its alloys: the materials and biological issue. ASTM SP 1272, West Conshohocken, 1996, p. 240.
3. ELIAS, L. M., SCHNEIDER, S. G., SCHNEIDER, S., SILVA, H. M., MALVISI, F, Mat. Sci. Eng. A **432**, (2006), p. 108.
4. NIINOMI, M., HATTORI, T., MORIKAWA, K., KASUGA, T., SUZUKI, A., FUKUI, H., NIWA, S., Mater. Trans. **43,** (2002), p. 2970.
4. CHEN, Y.Y., XU, L.J., LIU, Z.G., KONG, F.T.,CHEN, Z.Y., Trans. Nonferr. Metal Soc. **16**, (2006), p. 824.
5. XU, L.J., XIAO, S.L., TIAN, J., CHEN, Y.Y., HUANG, Y.D., Trans. Nonferr. Metal Soc. **22**, (2012), p.639
7. CHENG, Y., HU, J., ZHANG, C., WANG, Z., HAO, Y., GAO, B, J.Biomed. Mater. Res. B. Appl. Biomater. **101**,(2013), p.287.
8. KHAN, M. A., WILLIAMS, R. L., WILLIAMS, D. F., Biomaterials, **17**,(1996), p. 2117.
9. GROSGOGEAT, B., RECLARU, L., LISSAC, M., DALARD, F., Biomaterials, **20**, (1999), p. 933-941.
10. CHELARIU, R., BOLAT, G., IZQUIERDO, J., MARECI, D., GORDIN D.M., GLORIANT ,T., SOUTO, R.M., Electrochim. Acta, **137**, (2014), p. 280.
11.ALKHATEEB, E., VIRTANEN, S., J. Biomed. Mater. Res. A, 75 (2005), p. 934.

12. *** ASTM E384: Standard Test Method for Knoop and Vickers Hardness of Materials
13. *** ISO 6507-1: Metallic materials – Vickers hardness test – Part 1: Test method
14. *** ISO 6507-2: Metallic materials – Vickers hardness test – Part 2: Verification and calibration of testing machines
15. *** ISO 6507-3: Metallic materials – Vickers hardness test – Part 3: Calibration of reference blocks
16.*** ISO 6507-4: Metallic materials – Vickers hardness test – Part 4: Tables of hardness values
17. *** ISO 18265: Metallic materials – Conversion of Hardness Values
18. CVIJOVIC-ALAGIC, I., CVIJOVIC, Z., BAJAT, J., RAKIN, M., Corros. Sci., **83** (2013), p. 245.
19. IZQUIERDO, J., BOLAT, G., MARECI, D., MUNTEANU, C., GONZALEZ, S., SOUTO, R.M., Appl. Surf. Sci., **313** (2014), p. 259.
20. MATEI, M.N., CHISCOP, I., EARAR, K., MOISEI, M., MARECI, D., TRINCA, L.C., STAN, T., MUNTEANU, C., PACURAR, M., ILIE, M., Rev. Chim.(Bucharest), **66**, no. 12, 2015, p. 2009
21. BARCA, E.S, TRINCA, L.C, FILIPESCU, M., DINESCU, M., PLÃIA ª U, A.G., ABRUDEANU, M., LEATA, R., Rev. Chim. (Bucharest), **67**, no. 1, 2016, , p. 177
22. IACOBAN, S., BOLAT, G., MUNTEANU, C., CAILEAN, D., TRINCÃ, L.C., MARECI, D., Rev. Roum. Chim. 60(10), (2015), p. 949
23. MATEI, M.N., EARAR, K., MARECI, D., TRINCA, L.C., MARECI, D., FOTEA, L., PEPTU, C.A., BICA, C., Rev. Chim. (Bucharest), **67**, no. 4, 2016, p. 800
24. ROMAS, M., MARECI, D., SUTIMAN, D., TRINCÃ, L.C., STRUGARIU, S.I., MUNTEANU, C., 2015, Env. Eng. Manag. J. 14 (11), p. 2719
25. ISTRATE, B., MARECI, D., MUNTEANU, C., STANCIU, S., CRIMU, C.I., TRINCA, L.C., EARAR, K.., Env. Eng. Manag. J. 15 (5), (2016), p. 9
26. STANCIU S., URSANU A., TRINCA L. C., TROFIN A. E., SOLCAN C., MUNTEANU C., CIMPOESU N., ACATRINEI D., SINDILAR E. V., STANCIU T., FANTANARIU M., TOPLICEANU L., Env. Eng. Manag. J., 15, 5, p. 973
27. RONDELLI, G., VICENTINI, B., Biomaterials, **23** (2002), p. 639.
28. SOUTO, R.M., ALANJALI, M., Corr Sci, **42** (2000), p. 2201.
29. BROWNE, M., GREGSON, P.J., Biomaterials, **15**, (1994), p. 894

Manuscript received: 20.12.2106